

Muon angles at sea level from cosmic gamma rays below 10 TeV

J. Poirier¹, S. Roesler², and A. Fassò³

¹Center for Astrophysics at Notre Dame, Physics Dept., University of Notre Dame, Notre Dame, Indiana 46556 USA

²Stanford Linear Accelerator Center, Stanford, California 94309, USA

³CERN-EP/AIP, CH-1211 Geneva 23, Switzerland

Abstract. The FLUKA Monte Carlo program is used to predict the angular distributions of the muons which originate from primary cosmic gamma rays and reach sea level. This yields the inherent angular resolution of any instrument utilizing muons to infer properties of gamma ray primaries. Various physical effects are also discussed which affect these distributions in differing proportions.

1 Introduction

Muons detected at ground level arise mainly as decay products of charged mesons. These mesons are created abundantly in hadronic showers of primary cosmic ray protons and nuclei interacting inelastically with the nuclei of the atmosphere. A small fraction of muons, however, have their first origin in photonuclear reactions of primary cosmic gamma rays. Despite their relative scarcity compared to the large background of muons from hadron-generated showers, muons originating from primary gamma ray interactions are important for ground-based high statistics cosmic ray experiments sensitive to energies ≤ 10 TeV such as MILAGRO (2000) and GRAND (Poirier et al. (1999)). Cosmic gamma rays, unlike charged hadrons, are unaffected by magnetic fields and their direction points directly to the location of their source. Therefore, an accumulation of muon angles around a particular angle (and also at a particular time in the case of pulsed sources or gamma ray bursts) carries direct information about the location of the source and the neutrality of the primary causing the excess.

The information about the primary gamma direction is degraded by multiple physical processes so the final measured direction of the secondary muon is no longer collinear with the primary gamma. The angular resolution is affected by the angle of production of the mesons in the primary and subsequent interactions, the decay angle of the muon relative to its parent meson, Coulomb scattering, and deflection in the

Earth's magnetic field. These effects depend upon the energy of the primary, on various properties of the atmosphere such as pressure and temperature, etc.

The present study is to calculate the influence of these various effects on the ultimate angular resolution which can be obtained utilizing ground level muons. The Monte Carlo program FLUKA (Fassò et al., 1997a,b, 2000a,b) provides an accurate and well-tested description of the hadronic and electromagnetic interactions with all the relevant physical effects. The physical models implemented in FLUKA which are relevant for the present study as well as added details to the present paper are discussed in Fassò et al. (2001). Only incident cosmic gamma rays at perpendicular (vertical) incidence on top of the atmosphere are considered. Ground-based experiments often choose angles close to normal for reasons of simplicity and because the detection rate is maximum. For small angles from normal, the angular resolution results will probably not differ significantly from those presented in this paper.

2 Monte Carlo simulation of gamma ray showers

In order to study the dependence of the shower properties on the primary photon energy, the showers were calculated for monoenergetic photons impinging vertically on top of the atmosphere (taken to be 80 km above sea level). Primary energies of 1, 3, 10, 30, 100, 300, 1000, 3000, and 10000 GeV were studied. The atmosphere was approximated by 50 layers of constant density with the layer-density decreasing exponentially with altitude as in Fassò et al. (2001). The geometry has its origin at the intersection of the shower axis with sea-level, z is down, x is North, and y is East.

The effect of the Earth's magnetic field is discussed later as it depends on geographical location. Fig. 1 summarizes the deviations of the angle of the muons which reach sea level from the primary gamma direction (vertical angle). It shows the distribution of the angle Θ_{xz} which is the muon's angle with respect to the z axis projected onto the xz plane (North-down plane). Negative projections have been reflected upon

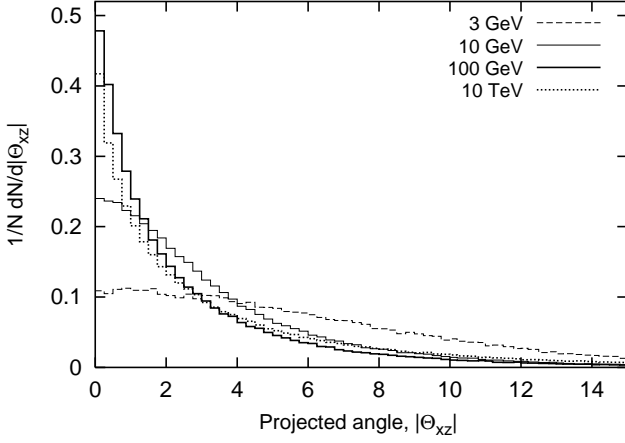


Fig. 1. Angular distribution of muons at sea level. Θ_{xz} is the angle of the detected muon projected onto the North-down or xz plane. The distributions are given for different primary photon energies and are normalized to unit area. Effects of the Earth's magnetic field are not included in this figure. Units of angle are in degrees.

the positive values because of symmetry in the absence of a magnetic field. Similarly, the distributions in the yz plane (East-down plane) are the same as those shown in Fig. 1. Since the angle of the primary gamma with respect to the z axis is zero, the results shown in Fig. 1 thus represent the correlation between the direction of the detected muon and the direction of the primary gamma ray.

All distributions in Fig. 1 are normalized to unit area to compare shapes. The shape of the distributions for primary energies above about 30 GeV varies rather slowly where histograms at 100 GeV and 10 TeV are shown. Below 30 GeV energy, the shape of the distributions changes significantly as can be seen from the histograms at 3 and 10 GeV. The distributions become wider with decreasing primary energy below 30 GeV. At low primary gamma ray energies, the muons have, on average, lower energies causing larger angular deviations due to kinematics and scattering effects which are larger for the lower energies.

Table 1 gives two measures of the widths of these distributions as a function of the energy of the incident primary cosmic gamma ray. The width parameters are: the half-width at half-maximum-height (hwhm) and the half-width containing 68% of the muons, i.e., the same number of events that a 1σ cut would include if the distributions had a Gaussian shape (which lacks the long tails). Both of these parameters provide a measure of the distribution widths which minimizes the distorting effect of a tail. Values for various cuts on the kinetic energy of the detected muons (0, 1, 2, and 4 GeV) are presented. The cutoff energy results for primary energies below 10 GeV were omitted due to lack of statistics. Numbers for $\Delta\Theta_{yz}$ are the same as $\Delta\Theta_{xz}$ from symmetry. The x and y rectangular coordinate system was chosen to represent the results of the muon's angular distribution as the corrections for the additional deflection due to the Earth's magnetic field differ in these two directions. In addition, (x, y) is a natural coordinate system for GRAND. For some experiments a space

Table 1. Half-width at half-maximum-height ($\delta\Theta_{xz}$ (hwhm)) of the angular distributions and angular half-width containing 68% of the muons ($\delta\Theta_{xz}$ (68%)); units are degrees. Values are given for muon energies above 0, 1, 2, and 4 GeV. The Earth's magnetic field has been neglected.

E_γ	$\delta\Theta_{xz}$ (hwhm)			
	$E_\mu > 0$	$E_\mu > 1$	$E_\mu > 2$	$E_\mu > 4\text{GeV}$
1	31.0	—	—	—
3	8.20	—	—	—
10	3.23	2.95	2.57	1.87
30	1.87	1.73	1.59	1.35
100	1.12	1.04	0.95	0.81
300	0.92	0.85	0.77	0.66
1000	0.91	0.82	0.74	0.63
3000	0.98	0.89	0.78	0.66
10000	1.05	0.94	0.82	0.67
1	$\delta\Theta_{xz}$ (68%)			
	28.3	—	—	—
3	7.36	—	—	—
10	3.83	3.06	2.46	1.66
30	3.07	2.40	1.95	1.45
100	2.87	2.15	1.69	1.21
300	3.04	2.18	1.68	1.16
1000	3.32	2.31	1.75	1.19
3000	3.62	2.42	1.81	1.23
10000	4.05	2.57	1.89	1.27

angle is more natural. If we define $R = \sqrt{x^2 + y^2}$, then the space angle resolution ($\delta\Theta_R$) can be estimated directly from the numbers in Table 1 by multiplying these values by $\sqrt{2}$ due to the symmetry between x and y in the absence of a magnetic field.

As can be seen in this Table 1: (i) as the primary energy decreases below 10 GeV, the width of angular distribution increases dramatically, (ii) as the energy rises above 300 GeV, there is only a small, gradual increase in the width of the angular distribution, and (iii) the width of the distribution narrows as the muon's cutoff energy is raised; i.e., the angular resolution improves by eliminating the lower energy muons which have, on average, poorer angular resolution.

The results of the preceding calculations can be combined to obtain the expected angular resolution for a spectrum of primary gamma rays. Various steps in the calculation are contained in Fig. 2. Here, a differential energy spectrum is assumed $d\Phi_\gamma/dE_\gamma \propto E_\gamma^{-\alpha}$ with a spectral index $\alpha=2.41$ corresponding to an average of the spectral indices reported in the Third EGRET Catalog (Hartman et al. (1999)). Folding $d\Phi_\gamma/dE_\gamma$ with the number of muons reaching sea level per primary photon, N_μ/N_γ , yields the number of muons at sea level as a function of the primary gamma ray energy, $d\Phi_\mu/dE_\gamma$, with $\Phi_\mu = N_\mu/N_\gamma \times \Phi_\gamma$.

The flatness of the differential muon flux per gamma at sea level ($E_\gamma \times d\Phi_\mu/dE_\gamma$) above 10 GeV signifies that the muons originate rather uniformly from a broad range of primary energies. Below 10 GeV, the muon flux decreases steeply

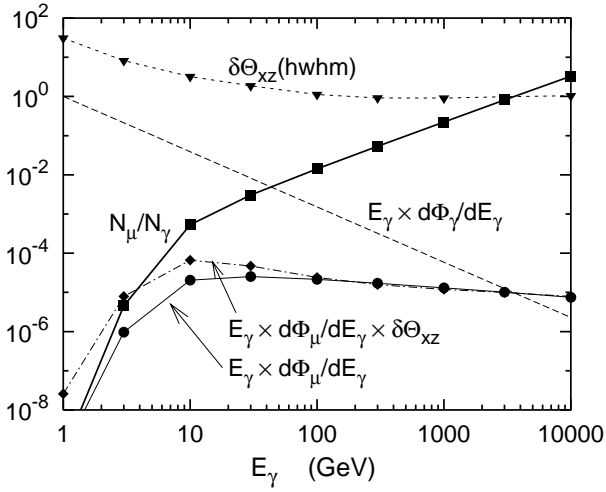


Fig. 2. The figure shows the following quantities as a function of the primary gamma ray energy: the energy spectrum of primary gamma rays ($d\Phi_\gamma/dE_\gamma$) with a shape given by a differential spectral index $\alpha = 2.41$ and arbitrary normalization, the multiplicity of muons at sea level per primary gamma ray (N_μ/N_γ), the result of folding the multiplicity with the primary spectrum ($d\Phi_\mu/dE_\gamma = N_\mu/N_\gamma \times d\Phi_\gamma/dE_\gamma$; thin solid line with circles), the half-widths at half-maximum-height for all muon energies ($\delta\Theta_{xz}$ (HWHM)) in degrees, and the result of folding these widths with $d\Phi_\mu/dE_\gamma$ (dot-dashed lines with diamond points). The calculated values are joined by lines to guide the eye. Note that all differential fluxes are multiplied by E_γ .

as N_μ/N_γ rapidly approaches zero. Harder spectral indices ($\alpha < 2.41$) would enhance the muon flux from higher primary energies and, conversely, softer indices would enhance lower energies.

Furthermore, in Fig. 2 the half-widths at half-maximum-height $\delta\Theta_{xz}$ (hwhm) (given in Table 1 in the “all E_μ ” column) are plotted. These widths are multiplied by the differential muon flux which is also shown in Fig. 2. As can be seen, the larger angular widths at the lower energies ($E_\gamma < 3$ GeV) do not contribute due to the small sea level muon flux at these energies.

The average angular resolution (i.e., average angular width) in the North-down plane, $\langle\delta\Theta_{xz}(\text{hwhm})\rangle$, for a differential gamma ray spectrum with an index α is obtained from

$$\langle\delta\Theta_{xz}(\text{HWHM})\rangle = \frac{\int \delta\Theta_{xz} \times N_\mu/N_\gamma \times E_\gamma^{-\alpha} dE_\gamma}{\int N_\mu/N_\gamma \times E_\gamma^{-\alpha} dE_\gamma} \quad (1)$$

shown in Fig. 3. The resolution is $\sim 1^\circ$ up to a spectral index of 2 and then rises for larger indices due to the importance of wider angular widths at low energy.

2.1 Effect of the magnetic field

The magnetic field of the Earth deflects positively (negatively) charged particles primarily eastward (westward) causing the angular distributions in the projected angle Θ_{yz} (i.e., projected onto the East-down plane) to become wider. The size of the effect depends on the strength and direction of the

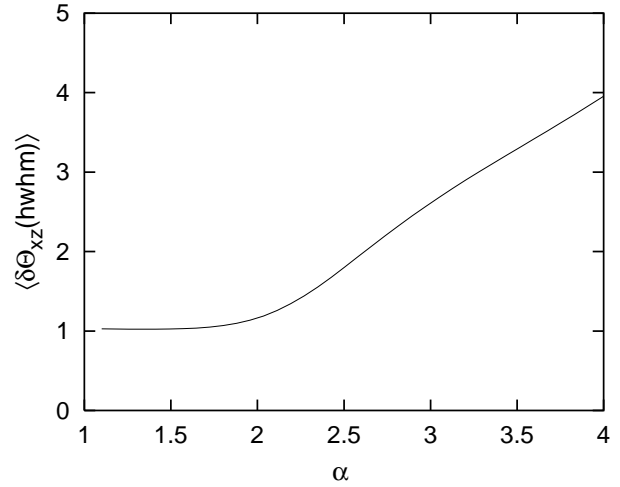


Fig. 3. Average half-width at half-maximum-height for the angle projected onto the North-down plane as a function of the spectral index (α) of the primary spectrum in degrees. Values for the space angle resolution ($\delta\Theta_R(\text{hwhm})$) would be $\sqrt{2}$ times larger.

field and, therefore, varies with geographic location. In addition to the previous case of no field (n.f.), three non-zero magnetic field values were considered: (1) $B_x = 0.186$ Gauss at 42°N , 86°W (GRAND), (2) $B_x = 0.228$ G at 36°N , 106°W (MILAGRO), and (3) $B_x = 0.414$ G at 9°N , 100°E (maximum possible); see IAGA (2000). For uniformity of comparison, all values are for sea level. Since the variation of the field in the atmosphere with height above sea level and with time is only minor (about 4%), for simplicity the magnetic field for a certain location was assumed to be constant from 0 to 80 km. In addition, although the MILAGRO experiment is located at 2170 m above sea level, all results reported for that location refer to sea level as this allows a direct comparison to the results at the other locations.

The angular distributions at sea level for no magnetic field (no field) and for three increasing values of magnetic field for primary gamma ray energies of 10 GeV are shown in Fig. 4. For a 10 GeV gamma, the effect of the Earth’s magnetic field is considerable, becoming larger as the northward (x) component of the magnetic field increases. The angular distribution at 1 TeV is much narrower and shows correspondingly less effect upon the magnetic field deflection.

The widths of the angular distributions in the North-down (Θ_{xz}) and East-down planes (Θ_{yz}) containing 68% of the muons are presented for the different locations in Table 2. Again, the widths are given for distributions containing only muons above certain kinetic energy thresholds (including zero threshold). In addition, the corresponding values from the calculations without the effect of the magnetic field are given. The widths in the North-down plane are much less affected than in the East-down plane which contains the dominant effect of the magnetic deflection. This effect increases with increasing values of B_x or decreasing values of muon momentum. In addition to the widths of the muon’s sea level angular distributions, Table 2 also shows the values at their

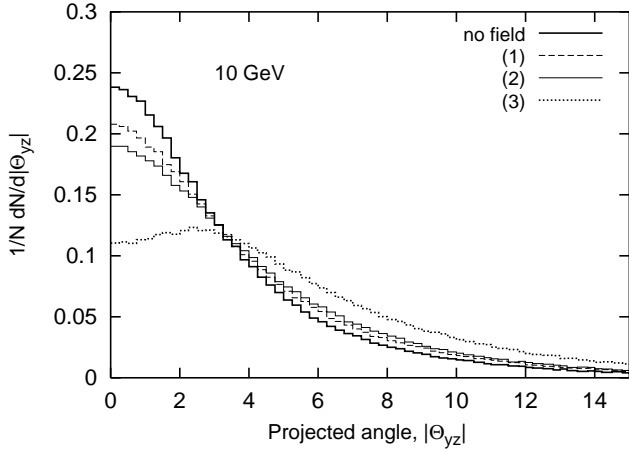


Fig. 4. Muon angular distribution at sea level including the effect of the Earth’s magnetic field for 10 GeV primary gammas. The distributions of the muon’s angle projected onto the yz (East-down) plane, Θ_{yz} , are shown (in degrees) for no (magnetic) field, and for three values of increasing B_x (defined in the text).

production vertex (birth, E-d.(b)). Interestingly, these values are almost constant for the different field conditions showing negligible magnetic deflection of the muon’s progenitors due to their shorter path lengths and higher momenta. The effect of the magnetic field on the angular distributions is therefore mainly the deflection of the muon. The dominant factor in the final width (except for the highest magnetic field value) is the muon’s angular distribution at its production (birth) point.

2.2 The effect of pressure and temperature variations

Air pressure and temperature changes cause a variation in the density profile of the atmosphere and thus affect the muon flux at sea level. A pressure increase was studied by increasing the air density in each layer by 3% while all other variables were kept constant and a temperature increase was studied by increasing the height of each slab boundary by 5% and decreasing the density by 5% thus keeping the total thickness of air constant. The mean temperature of a column of air 80 km high has a poor correlation with surface temperature; thus the temperature effect calculated here would require an averaged temperature over this column. These results allow corrections for the muon flux due to small variations in the air pressure and temperature. To summarize these results: a +1% increase in absolute air pressure causes a $-1.3 \pm 0.2\%$ change in muon rate at 10 GeV ($-1.1 \pm 0.2\%$ at 1 TeV); a +1% increase in absolute (Kelvin) temperature averaged from 0 to 80 km changes the muon rate by $-1.1 \pm 0.1\%$ at 10 GeV ($-0.7 \pm 0.1\%$ at 1 TeV).

Conclusions

Air showers caused by cosmic gamma rays with energies below 10 TeV were simulated using the Monte Carlo code FLUKA. The precise calculation of the angular correlations calculated in this paper provides experiments which study the angular location of primary gamma ray sources by measur-

Table 2. The half-widths of the muon’s sea level angular distributions which contain 68% of the muons in degrees. Results are presented for: (n.f.) no magnetic field (previous calculation) followed by increasing values B_x [(1), (2), and (3)]. For each location the half-widths are given for the projected angles onto the East-down (labeled “E-d.”) planes for primary gamma ray energies of 10 and 1000 GeV. Widths are listed for muon kinetic energies above 0, 1, 2, and 4 GeV. The second column under $E_\mu > 0$ gives the widths in the East-down plane of the muons at birth (labeled “b”).

	E_γ	$E_\mu > 0$		$E_\mu > 1$	$E_\mu > 2$	$E_\mu > 4$
		E-d.	E-d(b)	E-d.	E-d.	E-d.
n.f.	10	3.84	3.41	3.06	2.45	1.64
	1000	3.32	3.03	2.30	1.74	1.19
(1)	10	4.41	3.38	3.53	2.88	2.03
	1000	3.48	3.00	2.42	1.84	1.26
(2)	10	4.73	3.40	3.83	3.15	2.25
	1000	3.61	3.02	2.52	1.91	1.30
(3)	10	6.44	3.38	5.28	4.44	3.34
	1000	4.19	3.02	2.93	2.24	1.56

ing muon angles with information on the angular resolution which is difficult to obtain experimentally.

Acknowledgements. Part of this work was supported by the Department of Energy under contract DE-AC03-76SF00515; Project GRAND is funded through grants from the University of Notre Dame and private donations.

References

- A. Fassò *et al.*, in *Proceedings of the 2nd Workshop on Simulating Accelerator Radiation Environments, CERN 1995*, edited by G.R. Stevenson, CERN Report TIS-RP/97-05, p. 158 (1997).
- A. Fassò *et al.*, in *Proceedings of the 3rd Workshop on Simulating Accelerator Radiation Environments, KEK 1997*, edited by H. Hirayama, KEK Proceedings 97-5, p. 32 (1997).
- A. Fassò, A. Ferrari, and P. R. Sala, *Electron-photon Transport in FLUKA: Status*, to appear in *Proceedings of the International Conference on Advanced Monte Carlo for Radiation Physics, Particle Transport Simulation and Applications, Monte Carlo 2000*, Lisbon, Portugal, 2000.
- A. Fassò *et al.*, *FLUKA: Status and Perspectives for Hadronic Applications*, to appear in *Proceedings of the International Conference on Advanced Monte Carlo for Radiation Physics, Particle Transport Simulation and Applications, Monte Carlo 2000*, Lisbon, Portugal, 2000.
- A. Fassò and J. Poirier, *Phys. Rev. D* **63**, 036002 (2001).
- R. C. Hartman *et al.*, *Astrophys. J. Suppl. Ser.* **123**, 79 (1999).
- International Association of Geomagnetism and Aeronomy (IAGA), Division V, Working Group 8, *International Geomagnetic Reference Field - Epoch 2000, Revision of the IGRF for 2000 - 2005*, World Wide Web: <http://www.ngdc.noaa.gov/IAGA/wg8/wg8.html>
- The MILAGRO Collaboration, R. Atkins *et al.*, *Nucl. Instr. Meth. in Phys. Res. A* **449**, 478 (2000).
- J. Poirier *et al.*, in *Proceedings of the 26th International Cosmic Ray Conference (ICRC)*, Vol. 5, p. 304 (1999), World Wide Web: <http://www.nd.edu/~grand>.